Characterization of the Gonioapparent Character of Colored Anodized Titanium Surfaces

Renée Charrière,[1]* Grégoire Lacaille,[1] Maria Pia Pedeferri,[2] Jenny Faucheu,[1] David Delafosse[1]

[1]Ecole Nationale Supérieure des Mines de Saint-Etienne, SMS EMSE, CNRS UMR5307, Laboratoire Georges Friedel, 158 cours Fauriel, 42023 Saint-Etienne, France

[2]Department of Chemistry, Materials and Chemical Engineering, "Giulio Natta" Politecnico di Milano, via Mancinelli 7, 20131 Milano, Italy

Received 2 April 2014; revised 20 July 2014; accepted 30 July 2014

INTRODUCTION

Titanium oxidation has been widely investigated in the literature for its particular physical properties giving rise to a large range of industrial applications. Titanium dioxide (TiO_2) may not only exhibit, for example, interesting photocatalytic properties[1,2] useful for antifogging or surface self-cleaning application[3,4] but also an interferential coloration[5] well appreciated by architects or designers. Titanium oxidation can be performed in many ways, for example, by anodizing,[6] laser irradiation,[7] or heating.[8] Coloration of titanium may be obtained from all these techniques, and the set of achievable colors is sufficiently wide to consider these techniques suitable for jewel creation.[9,10]

In this study, we focus on coloration of commercial titanium plates by anodic oxidation. The thickness of the oxide layer formed at the surface of the metal is in the same range as visible wavelengths. The colors are generated by a multiwave interference phenomenon occurring between light reflected by the air/oxide interface and light transmitted by this interface and performing one or multiple reflections inside the oxide layer before being again transmitted by the interface. The interference is destructive for some wavelengths in the visible range, leading to the coloration of the material. The destructive interference condition depends on the optical path difference between light rays, which varies with the oxide layer thickness, the oxide refractive index, as well as with the incident light direction. For a perfectly flat surface, the observed color is thus expected to vary with the illumination direction. Colors of anodized titanium plates have been already characterized[11,12] and efficiently predicted by a two-wave interference model considering smooth parallel interfaces.[11] However, although they are commonly observed, variations of these colors with the directions of illumination or observation have not been studied quantitatively. Furthermore, a two-wave model, such as proposed by Diamanti *et al.*,[11] can neither render nor predict color variations with the observation or illumination angle. A more complete modeling of interference effects in a nonplanar oxide layer would indeed be useful to rationalize why

*Correspondence to: Renée Charrière (e-mail: renee.charriere@emse.fr)

TABLE I. Characteristics, surface preparation, and denomination of the samples.

Denomination	Material	Sample thickness (mm)	Initial surface finishing	Surface preparation	R_a (μm)	S_{dq} (°)
Series 1	Grade 1	2	Smooth	Mirror polishing	0.15	7.5
Series 2	Grade 2	1.3	Rough	No preparation	1.9	17.5
Series 3	Grade 2	2	Smooth	No preparation	0.33	15.4
Series 4	Grade 2	2	Smooth	Mirror polishing	0.15	7.5

The mean roughness parameter R_a and the root mean square surface slope S_{dq} were measured with an optical profiler Wyko NT9100, ex Veeco, Bruker Nanoscope™.

some colors of anodized titanium are more prone than others to goniochromaticity, as well as to predict the degradation of color rendering with a physicochemical degradation of the oxide scale itself. This kind of complete electromagnetic modeling is beyond the scope of this study, but should undoubtedly rely on accurate measurements of the gonioapparent character of these colors. The aim of this study is to propose an experimental procedure to assess and quantify the goniochromatic character of anodized titanium surfaces with varying surface roughness. It relies on a goniospectrophotometer specifically designed to investigate gonioapparent and specular surfaces.[13]

In this work, we performed angular-dependent color characterizations of anodized titanium samples, with three different surface finishes from "as received" (denoted "rough" in the following) to mirror polished. In the following sections, we will first describe the anodizing process and the different surface properties. The color variations measurement method will then be presented and the results will be discussed.

SAMPLE REALIZATION AND SURFACE CHARACTERIZATION

The anodized samples were 3 cm × 4 cm coupons sampled in commercial-grade pure titanium plates (ASTM grade 1 or 2). Two types of grade 2 plates were used: the first one is 1.3 mm thick and had initially a rather rough surface before preparation; the second one was smoother, with a thickness of 2 mm. The grade 1 plate was 2 mm thick, with a relatively smooth surface topology.

Different surface preparations have been carried out on the samples as presented in Table I, where the denomination of the various samples is also mentioned. The average roughness R_a and the root mean square surface slope S_{dq} indicated in Table I were measured with an optical profiler Wyko NT9100, ex Veeco, Bruker Nanoscope™. These parameters are defined by the following equations:

$$R_a = \frac{1}{S}\int_S |Z(x,y)|\,dxdy, \tag{1a}$$

$$S_{dq} = \sqrt{\frac{1}{S}\int_S \left[\left(\frac{\partial Z(x,y)}{\partial x}\right)^2 + \left(\frac{\partial Z(x,y)}{\partial y}\right)^2\right] dxdy}\ , \tag{1b}$$

where S is the scanned surface and $Z(x,y)$ the difference between the elevation of the surface and its average elevation.

The mirror polishing is obtained by applying successively a silicon carbide grinding paper P240, 9 μm to 1 μm diamond paste suspensions, and 0.25 μm colloidal silica suspension for final polishing.

After degreasing with acetone, the samples are anodized in 0.5 M sulfuric acid, with a galvanostatic regime current of 6 A. The applied potential is equal to 10, 20, or 90 V to generate different oxide layer thicknesses[5] and thus different colors. The current–voltage generator used for anodizing is a MicroLab MX 200V-12A.

The mirror-polished samples were also characterized in a Scanning Electron Microscope Zeiss Supra 55. Figure 1 displays a SEM image of the surface of the 90 V sample of series 4 (see Table I). The oxide layer is fairly homogeneous, with no clearly apparent porous structure. Some submicrometer craters are present on the surface due to the anodizing process at 90 V; however, the dimension of the craters is of the same order of R_a (the craters are not present for an anodizing potential of 20 V).

Figure 2 presents digital colored pictures of the anodized samples with an observation angle either equal to or different from the incidence angle of light, which corresponds to the "specular" and "out of specular" geometries, respectively.

At first sight, we observe that the color of the samples, for the same anodizing potential, may vary according to the surface finishing. This phenomenon is especially noticeable for the samples anodized at 90 V, which appear either pink in series 2 in the specular direction or green in series 4 in the same observation conditions. One may also notice that the color of the 90 V sample in

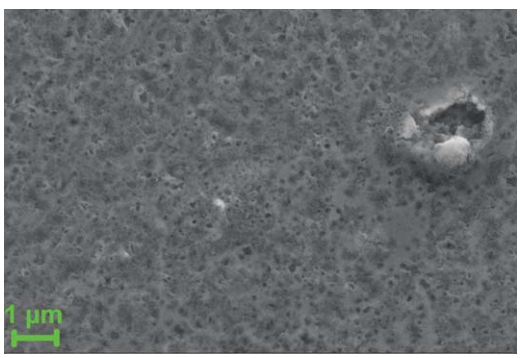

Fig. 1. SEM image of the surface of the 90 V sample of series 4.

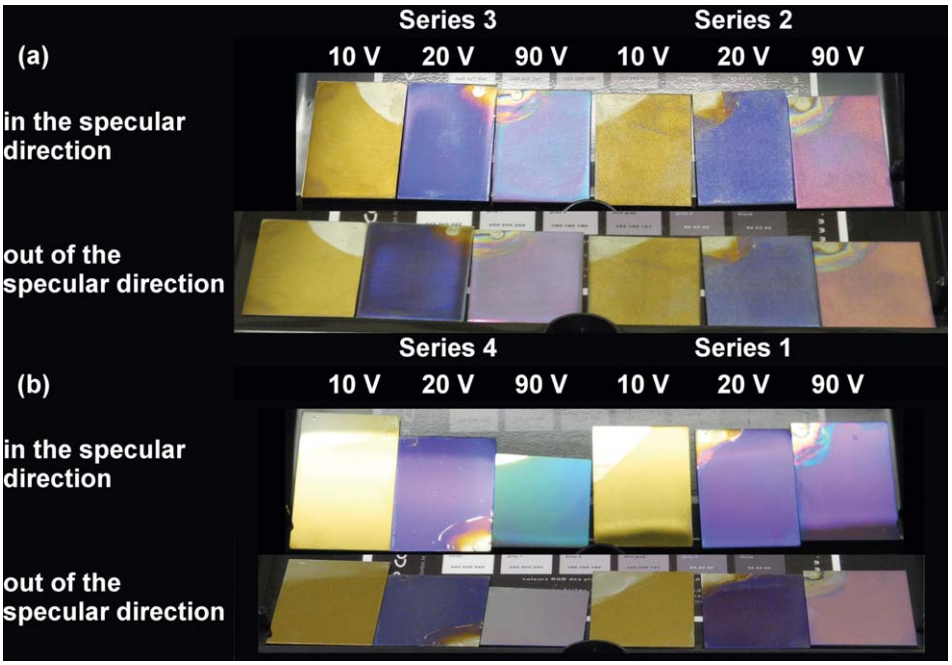

Fig. 2. Digital color pictures of the anodized samples of the series 2 and 3 (a) and of the series 1 and 4 (b). The incidence angle of the illuminant source is 45°, and the observation angle is either 45° (specular direction) or 70° (out of the specular direction).

series 1 appears pink in the specular direction, indicating that the anodizing process yields different oxide layer properties on grade 1 or grade 2 metallic plates.

All the samples do not have the same level of gonioappearance, that is, the same variation of color rendering according to the viewing angle. It is more pronounced for the 90 V samples in series 4, whereas the roughest samples (series 2) are almost not gonioapparent.

REFLECTANCE MEASUREMENT PROCESS AND COLOR COMPUTATION

To characterize more accurately the color variations illustrated in Fig. 2, we performed goniospectrophotometric measurements. These measurements have been conducted with the goniospectrophotometer OptiMines developed at Ecole des Mines de Saint-Etienne, which was specifically designed to investigate specular and gonioapparent samples.[13] The device is composed of three main subsystems:

- a rotating illumination arm containing a 50-W fibered halogen lamp, which illuminates the sample after been collimated by an optical system,
- a rotating and movable sample holder, and
- a rotating detection arm containing a second optical system which focuses the light beam reflected by the sample onto a fibered Maya2000 Pro spectrometer, with a spectral sampling interval of 0.5 nm and a spectral bandwidth of 3 nm.

The illumination and detection arms have only one rotational degree of freedom and move in the same plane. The sample holder has two rotational degrees of freedom: it may rotate on itself or tilt around the motion plane of the illumination and detection arms. The sample holder may also be moved back to allow the direct spectrometric measurement of the source.

The key features of this device are its high-angular positioning accuracy (less than 0.02°) and its low incident light half-divergence and detector's angular half-acceptance (both are equal to 0.1°), which make it very sensitive to rapid angular variations of the spectral reflectance.

The goniospectrophotometer enables measurements of the bidirectional reflectance distribution function (BRDF) of the samples. This function is defined[14] by the ratio of the spectral radiance $L_r(\theta_r, \phi_r, \lambda)$ reflected from a surface in a given viewing direction (θ_r, ϕ_r) to the spectral irradiance $E_i(\theta_i, \phi_i, \lambda)$ on the surface arising from an illuminant source in the incident direction (θ_i, ϕ_i):

$$BRDF(\theta_i, \phi_i, \theta_r, \phi_r, \lambda) = \frac{L_r(\theta_r, \phi_r, \lambda)}{E_i(\theta_i, \phi_i, \lambda)}, \tag{2}$$

where λ denotes the wavelength.

The BRDF measurements are performed in two steps: the first one consists of a direct measurement of the light flux F_{source} of the source, and the second one consists of a measurement of the light flux F_{sample} reflected by the observed sample. The experimental expression of the BRDF is then given by the following equation[13]:

$$BRDF(\theta_i, \phi_i, \theta_r, \phi_r, \lambda) = \frac{F_{sample}(\lambda,\ \theta_r, \phi_r)}{F_{source}(\lambda)\Omega_s \cos(\theta_i)}, \tag{3}$$

where Ω_s is the illumination solid angle.

To underline the high-angular positioning accuracy of our goniospectrophotometer, we present a repeatability

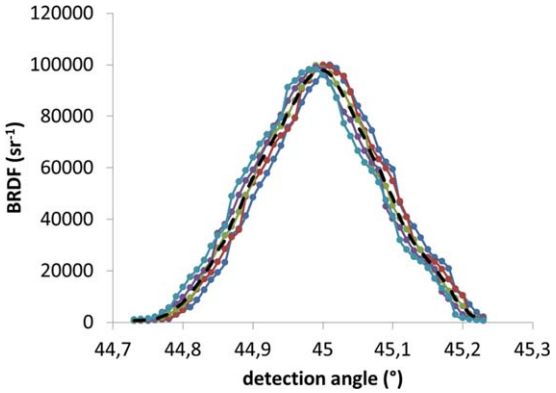

Fig. 3. Characterization of the detection arm angular positioning precision by means of a repeatability measurement with five acquisitions (colored curves) of the BRDF of an aluminum mirror around the specular direction in the incidence plane and for an incidence angle of 45°. The acquisition step is 0.01°. The represented BRDF data correspond to an average over 4 nm around a central wavelength of 700 nm. The black dashed curve represents the average of the five BRDF measurements.

characterization of the detection arm positioning in Fig. 3. A repeatability characterization of the source arm positioning will give similar results. This characterization consists of five acquisitions of the BRDF of an aluminum mirror, ±0.25° around the specular direction by 0.01° steps in the incidence plane and for an incidence angle of 45°. The represented BRDF data correspond to an average over 4 nm around a central wavelength of 700 nm. To quantify the precision of the angular positioning of the detection arm from this data, we calculate the average of the five BRDF measurements (represented as a black dashed curve in Fig. 3) and the corresponding standard deviation. The maximal value of the standard deviation over the angular range [44.75°; 45.25°] is denoted as $\sigma_{\max}$. We then calculate the maximal slope $\delta_{\max}$ of the average BRDF. The angular positioning precision δ_{θ_r} is then deduced in the following way:

$$\delta_{\theta_r} = \frac{\sigma_{max}}{\delta_{max}}. \quad (4)$$

From the data presented in Fig. 3, we obtain $\delta_{\theta_r} = 0.01°$.

The BRDFs of the anodized titanium samples were measured around the specular direction, in the incidence plane and in the visible spectral domain. Figure 4 displays the spectral BRDFs of the three samples of series 4, in the specular direction for an incidence angle of 45°, as a function of wavelength. The displayed spectra are typical of an interferential phenomenon, where the local minima of the spectra correspond to destructive interferences and the local maxima to constructive ones.

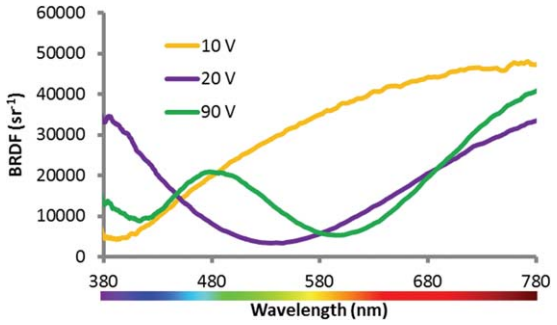

Fig. 4. BRDFs of the three samples of series 4 in the specular direction for an incidence angle of 45°.

From the spectral BRDF measurements, the (x, y) chromaticity coordinates as well as the luminance Y of the samples colors are computed, as defined in 1931 by the International Commission on Illumination (CIE),[15] considering a D65 illuminant. The conversion formulas from spectral BRDF to chromaticity coordinates are well known and can be found for example in Ref. [16]. The chromaticity values (x, y) are then represented in the CIE 1931 chromaticity diagram (e.g., see Fig. 6).

DESCRIPTION OF THE COLOR VARIATIONS CHARACTERIZATION METHOD

Many parameters may influence the spatial color variations of the samples. We have investigated this influence through many directions, and some examples illustrating its characteristic features are given in the "Results and Discussion" section. Two types of color evolutions are explored: the first one is the color evolution around the specular direction, and the second one is the evolution of the color in the specular direction for various incidence angles.

We first study the influence of the surface finishing on the color evolution around the specular direction. This is

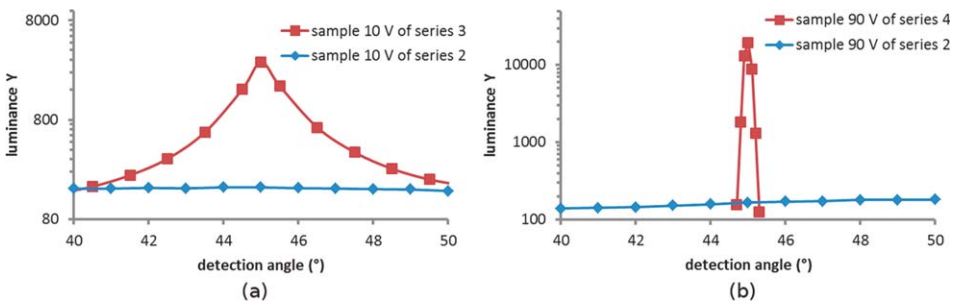

Fig. 5. Evolution around the specular direction of the luminance Y of the color of (a) the samples anodized at 10 V of series 2 and 3 and (b) the samples anodized at 90 V of series 2 and 4. The incidence angle is equal to 45°. Note that the Y scale is logarithmic.

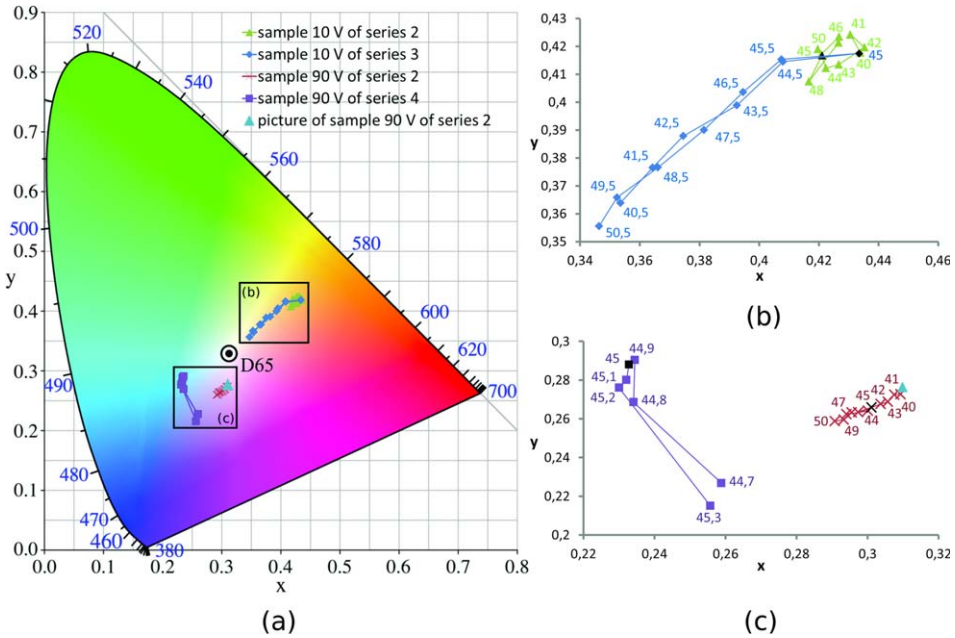

Fig. 6. (a) Evolution around the specular direction in the CIE chromaticity diagram of the colors of the samples anodized at 10 V of series 2 and 3 and the samples anodized at 90 V of series 2 and 4. The incidence angle is equal to 45°. The central surrounded black dot represents the D65 illuminant. Subfigures (b) and (c) corresponds to a zoom of the color evolution of (b) the samples anodized at 10 V and (c) the samples anodized at 90 V. The values indicated next to the data points on the graphs are the angular positions (in degrees) of the detection arm. For the sake of clarity of the graphs, not all detection arm positions are indicated. The blue triangle on the subfigures (a) and (c) corresponds to the (x, y) chromaticity coordinates of the 90 V sample of series 2 deduced from a colorimetrically calibrated digital picture of the sample in the specular direction and for an incidence angle of 45°. The black points on subfigures (b) and (c) indicate the specular direction.

illustrated here below, for an incidence angle of 45°, by two comparisons:

- the first one between the samples anodized at 10 V of series 2 and 3, and
- the second one between the samples anodized at 90 V of series 2 and 4.

We may observe that the rougher the surface, the weaker are the color variations in the chromaticity diagram. We thus focus in the following on the mirror-polished samples.

We then study the influence of the incidence angle on the color variations around the specular direction. This is illustrated on the sample anodized at 90 V of series 1 for four different incidence angles: 30°, 45°, 60°, and 70°. We observe that the more grazing the incidence angle, the weaker are the color variations. This study also shows the evolution of the color in the specular direction for the previously cited angles.

The rest of the study concerns only on the variations of the color in the specular direction for different incidence angles. These variations are explored through two parameters: the anodizing potential and the titanium composition (grade 1 or 2). This study is illustrated by measuring the sample color at three different incidence angles (45°, 60°, and 70°) at three different anodizing potentials (10, 20, and 90 V) for the series 1 (grade 1) and 4 (grade 2).

RESULTS AND DISCUSSION

The color variations of the samples are first investigated around the specular direction, for an incidence angle of 45°, regarding the influence of the surface roughness, for two different anodizing potentials, 10 and 90 V.

Figure 5(a) shows the variations of the luminance Y of samples anodized at 10 V from series 2 (very rough surface) and 3 (smooth surface) versus the detection angle. The luminance values of the rough sample are about 100 and exhibit weak variations with the detection angle, whereas the luminance values of the smooth sample are much higher than 100 near to the specular direction. Note that a luminance value greater than 100 means that, in the considered geometrical configuration, the sample reflects more light than a perfect white diffuser. This fact is a key problem for the definition of a color from BRDF measurements, especially if we characterize at the same time rough and specular samples, and illustrates the reason why we decided to represent the sample colors in the CIE chromaticity diagram, instead of other color spaces, for example CIE L*a*b*. The latter needs indeed to define a reference white point. The definition of a proper white point adapted for both specular and rough samples is under investigation.

Figure 5(b) shows the luminance variations of samples anodized at 90 V from series 2 (very rough surface) and 4 (mirror-polished surface) versus the detection angle.

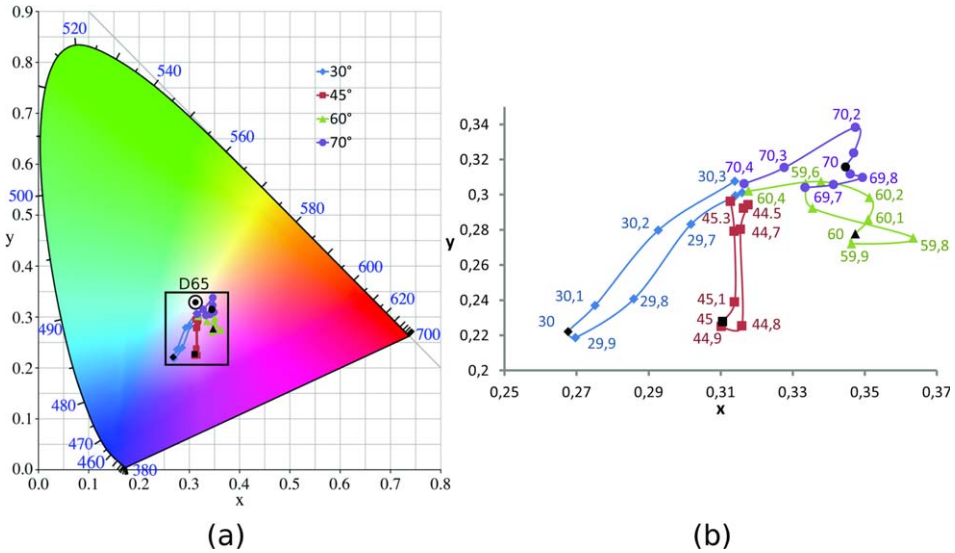

Fig. 7. Variation of the color of the 90 V sample of series 1 around the specular direction for various incidence angles: 30°, 45°, 60°, and 70°. The blackened points correspond to the specular direction. The subfigure (b) is a zoom of the black surrounded area of subfigure (a). The values indicated next to the data points on the subfigure (b) are the angular positions (in degrees) of the detection arm. For the sake of clarity of the graph, not all detection arm positions are indicated.

The same observations as for Fig. 5(a) can be made. It is worth noting that the highest luminance variations occur for the mirror-polished sample.

Figure 6 shows the color variations of the previous mentioned samples, in the CIE-chromaticity diagram, around the specular direction. We observe that for smooth or mirror-polished surfaces, the saturation of the color, evaluated here as the distance of the color to the D65 point, exhibit higher variations around the specular direction than for "rough" samples. The highest saturation variations occur for the most specular samples (10 V of series 3 and 90 V of series 4). Moreover, for these samples, the most saturated color corresponds to the specular direction, which is consistent with the interferential origin of the colors. In contrast, noninterferential-coated surfaces such as metallic plates with thick varnish coating would display, in the specular direction, a less saturated color due to the white light component reflected by the surface of the varnish.

Finally, the fact that the colors of the 10 V samples vary in the chromaticity diagram along almost straight lines passing through the D65 point means that the hue is almost invariant according to the observation angle for all surface roughness conditions. This is however not the case for the 90 V sample of series 4, which is consistent with the qualitative observation of the high gonioapparent character of this sample presented in Fig. 2.

To check our goniometric color measurements, we compared, for the samples of series 2, the (x, y) chromaticity values deduced from the goniometric measurements to those deduced from a colorimetrically calibrated picture. The picture is taken under a fluorescent lamp with a digital camera in the specular direction with an incidence angle of 45°. It is calibrated by introducing a 24-patches matte X-Rite ColorChecker® in the field of the camera. The calibration algorithm is a standard second-order polynomial regression,[17] which converts device-dependent RGB values to corrected XYZ components.

The (x, y) chromaticity values are then computed for each pixel, and one (x, y) chromaticity value is deduced from the image of each sample by averaging on an area of about 2 cm × 2 cm. These components are represented, for the 90 V sample, by a blue triangle in Fig. 6. We may consider that the sample color caught from the digital picture is in good agreement with the colors deduced from goniometric measurements given the following limiting factors. The illumination and detection solid angles are different for the goniometer and in the picture acquisition configuration, and the accuracy of the angular positioning of the camera is limited.

We will then characterize the evolution of the color around the specular direction for various incidence angles. Figure 7 presents this characterization for the series 1 sample anodized at 90 V at incidence angles equal to 30°, 45°, 60°, and 70°. For all values, we observe that the color with the highest saturation is in or very close to the specular direction. The specular color evolves from bluish to pinkish when the incidence angle increases and its saturation decreases. The hue modification reflects the gonioapparent character of the sample. The decrease of the saturation may be explained by the increase of the Fresnel reflection coefficient of the air/TiO_2 interface, which leads to a higher difference of amplitude between interfering light waves. The contrast of the interference fringes thus decreases, giving a spectral BRDF with less pronounced minima and maxima.

As the color saturation decreases in the specular direction with the incidence angle, we also observe that the saturation variations around the specular direction become weaker with an increase of the incidence angle.

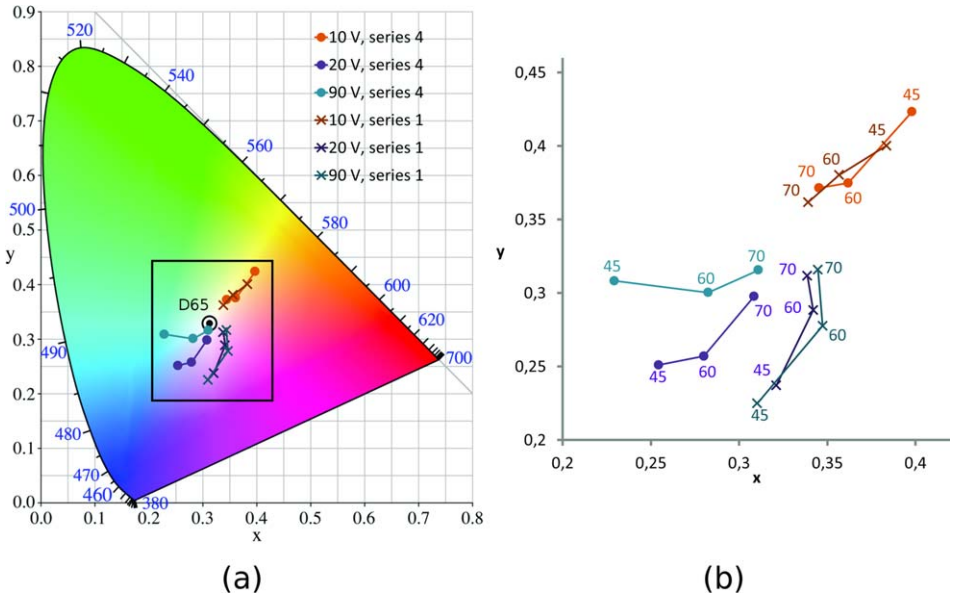

Fig. 8. Evolution of the color in the specular direction for the mirror-polished samples at incidence angles of 45°, 60°, and 70°. The subfigure (b) is a zoom of the black surrounded area of subfigure (a). The values indicated next to the data points on the subfigure (b) are the incidence angles. Note that the data presented in this figure for the 90 V sample of series 1 are the same as the blackened points of Fig. 6 for 45°, 60°, and 70°.

To quantify the gonioapparent character of the mirror-polished samples, the color in the specular direction for incidence angles of 45°, 60°, and 70° was measured (see Fig. 8). One can notice that for all samples, the previously mentioned decrease of the saturation of the sample color with an increase of the incidence angle is observed.

The gonioapparent character of a sample is quantified by computing the hue difference between the color in the specular direction at 45° and 70°. This hue difference, denoted as ΔH, is expressed in degrees and is computed as follows:

$$\Delta H = \frac{\operatorname{acos}\left(\overrightarrow{c_{45}} \cdot \overrightarrow{c_{70}}\right)}{\|\overrightarrow{c_{45}}\| \|\overrightarrow{c_{70}}\|}, \tag{5}$$

with $\overrightarrow{c_\alpha} = \begin{pmatrix} x_\alpha - x_{D65} \\ y_\alpha - y_{D65} \end{pmatrix}$, x_α and y_α being the (x, y) chromaticity values of the sample color in the specular direction for an incidence angle equal to α, and x_{D65} and y_{D65} the chromaticity values of the D65 white point. This ΔH value cannot be accurately linked to human color perception as it is not computed in a perceptually uniform space. It is computed here to give a quantitative comparison of the color evolution in the CIE chromaticity diagram between the different samples.

TABLE II. Values of the hue difference ΔH for the mirror-polished samples.

	Anodizing potential		
Series number	10 V	20 V	90 V
1	6°	51°	69°
4	5°	29°	69°

Table II gives the computed ΔH values for the mirror-polished samples characterized in this study. We can observe that the gonioapparent character of the samples increases with the anodizing potential. This evolution is in accordance with eye observations of the samples.

The measurements presented in Fig. 8 also represent a study of the color and gonioappearance difference between grade 1 and grade 2 titanium samples with same surface finishing. We observe that for a low anodizing potential (10 V), grade 1 and grade 2 samples exhibit very close colors, whereas the color difference between two grades is much higher at 90 V. To our knowledge, such a study has not been reported yet and offers the perspective to a further better comprehension of the difference in the anodizing mechanisms between these two titanium grades.

The range of colored effects that can be obtained through titanium anodizing is broad and depends on the nature of the base material, surface condition, and anodizing parameters. A systematic study of the gonioapparent character of these surfaces remains to be carried out.

CONCLUSIONS

Besides its excellent mechanical and physicochemical properties, the visual appearance of titanium can be tailored through anodizing. A wide gamut of structural colors can be obtained through well-defined surface preparation and anodizing conditions. The samples exhibit a gonioapparent character, depending on the surface structuration as well as on the anodizing potential. This gonioapparent character of anodized titanium however remains to be quantified.

We performed goniometric color characterizations of anodized titanium samples using a goniospectrophotometer

specifically designed for gonioapparent surfaces. They were cross-checked at observation angles corresponding to color saturation maxima by comparison with color measurements extracted from colorimetrically calibrated digital pictures obtained with comparable illumination and observation angles. This work opens the way toward mastering the angular color variations of anodized titanium. In general, gonioapparent color effects are difficult to characterize and quantify on a human-based perception scale, in part because of a lack of reference calibration maps, as it is the case for matte surfaces. Because of the wide range of goniochromatic effects which can be obtained and the high physicochemical stability of these surfaces, anodized titanium has the potential to serve as a base for developing such reference calibration maps for gonioapparent surfaces. Experimental BRDFs acquired on anodized titanium spheres were indeed used for the virtual prototyping of objects coated with pearlescent paint.[18] Thus, this article describes an experimental method to measure, quantify, and calibrate these effects.

ACKNOWLEDGMENTS

The authors thank Max Boudes and Gilles Blanc for sample preparation and Mathieu Hébert for fruitful discussions and careful proofreading of the paper.

1. Carp O, Huisman CL, Reller A. Photoinduced reactivity of titanium dioxide. Prog Solid State Chem 2004;32:32–177.
2. Ma Y, Qiu J-B, Cao Y-A, Guan Z-S, Yao J-N. Photocatalytic activity of TiO_2 films grown on different substrates. Chemosphere 2001;44: 1087–1092.
3. Wang R, Hashimoto K, Fujishima A, Chikuni M, Kojima E, Kitamura A, Shimohigoshi M, Watanabe T. Photogeneration of highly amphiphilic TiO_2 surfaces. Adv Mater 1998;10:135–138.
4. Nakajima A, Koizumi S, Watanabe T, Hashimoto K. Effect of repeated photo-illumination on the wettability conversion of titanium dioxide. J Photochem Photobiol A: Chem 2001;146:129–132.
5. Diamanti MV, Del Curto B, Ormellese M, Pedeferri MP. Photoactive and colored anodic oxides on titanium for architectural and design applications. Clean Technol 2008;1:170–173.
6. Pedeferri P. Method of coloring titanium and its alloys through anodic oxidation. Eur. Pat. 1,199,385–A2, 2000.
7. Pérez del Pino A, Fernández-Pradas J, Serra P, Morenza J. Coloring of titanium through laser oxidation: comparative study with anodizing. Surf Coatings Technol 2004;187:106–112.
8. Bartlett L. An unusual phenomenon observed when anodising CP titanium to produce coloured surfaces for jewellery and other decorative uses. Opt Laser Technol 2006;38:440–444.
9. O'Hana S, Pinkerton AJ, Shoba K, Gale AW, Li L. Laser surface colouring of titanium for contemporary jewellery. Surf Eng 2008;24:147–153.
10. Diamanti MV, Del Curto B, Masconale V, Passaro C, Pedeferri MP. Anodic coloring of titanium and its alloy for jewels production. Color Res Appl 2012;37:384–390.
11. Diamanti MV, Del Curto B, Pedeferri MP. Interference colors of thin oxide layers on titanium. Color Res Appl 2008;33:221–228.
12. Karambakhsh A, Afshar A, Ghahramani S, Malekinejad P. Pure commercial titanium color anodizing and corrosion resistance. J Mater Eng Perform 2011;20:1690–1696.
13. Matsapey N, Faucheu J, Flury M, Delafosse D. Design of a goniospectro-photometer for optical characterization of gonio-apparent materials. Meas Sci Technol 2013;24:065901.
14. Meyzonette JL, Lépine T. Bases de Radiométrie Optique. Toulouse: Cepadues; 2001.
15. CIE. E S 017/E:2011 ILV: International Lighting Vocabulary. Vienna: CIE Central Bureau, 2011.
16. Hunt RWG. Measuring Colour. Kingston-upon-Thames: Fountain Press; 1998.
17. Sharma G. Digital Color Imaging Handbook. Boca Raton: CRC Press LLC; 2002.
18. Kim DB, Seo MK, Kim KY, Lee KH. Acquisition and representation of pearlescent paints using an image-based goniospectrophotometer. Opt Eng 2010;49:43604–43613.